

# B-field Mapping Parameters

David Lawrence, Simon Taylor

March 27, 2013

## 1 Grid point spacing

To determine the maximum step size between points while mapping the solenoid field, the following method is used:

A map of the total field gradient is taken and at each point, the value of 200 Gauss is divided by the gradient ( $dB_{tot}/dx$ ) where  $x$  is in the direction of maximal gradient.

This results in a value that one can use to step in any direction and know that the field will not have changed by more than 200 Gauss. The value of 200 Gauss was chosen since it is approximately 1% of the field value in the interior region of the solenoid[1, 2, 3]. Figure 1 shows the gradient of the total B-field generated for the GlueX solenoid using the tool *bfield2root*. Figure 2 shows the calculated step sizes based on region inside the magnet.

Tables 1-5 give values of the desired measurement positions in  $z$  for when the probe is at various  $r$  values. For these values, a minimum step size of 1 cm and a maximum step size of 12 cm were imposed. Because the gradient is smaller at the center of the magnet, fewer points are needed there than at the outer edges. There are 660 measurement points total for these 4 radii. This number of measurements would be needed for each plane measured in the detector (e.g.  $0^\circ$ ,  $39^\circ$ ,  $45^\circ$ ,  $\dots$ ). Note that the outermost radius (32") the mapping only extends to  $z=350$  cm, or approximately the downstream location of the last coil. This was done because: 1.) The outermost radius is in a region that will be filled by the BCAL so tracking will not be done out to that radius. and 2.) The gradients of the field in that region are large and result in a very high measurement density. The reason for mapping this region is because it is so sensitive to the details of the geometry that it would provide a good comparison point with calculation.

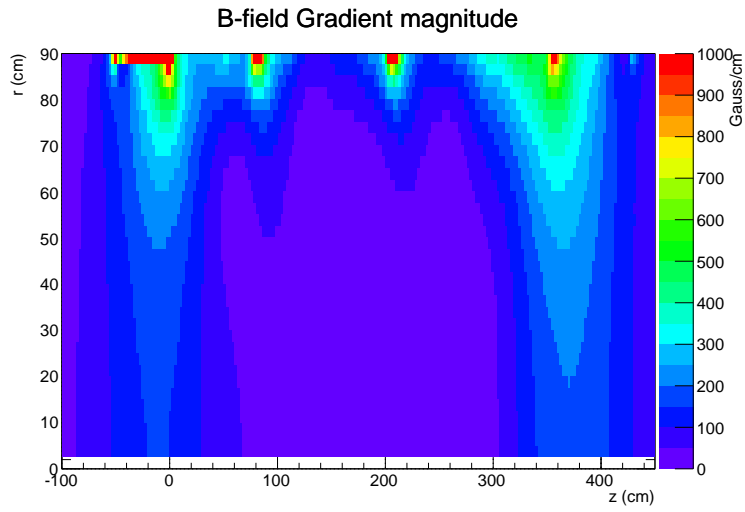


Figure 1: Gradient of the total B-field in the direction of greatest change.

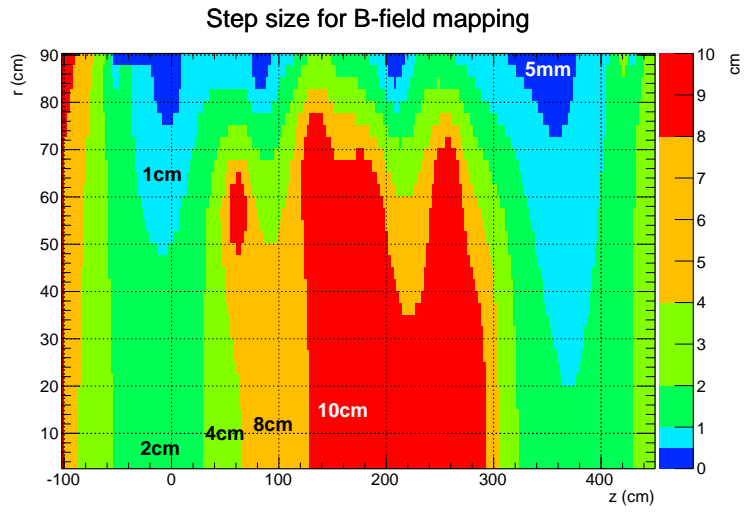


Figure 2: Estimated step size for B-field mapping by region.

Table 1: Measurement locations in Z for when probe is placed at r=0.0 cm (0 inches) from the beam line. Values are in cm and measured downstream along the beamline with zero being even with the upstream face of the most upstream coil in the magnet (see figure 6).

0.0 cm (0") - 123 points					
0 (+2cm)	2 (+2cm)	4 (+2cm)	6 (+2cm)	8 (+2cm)	10 (+2cm)
12 (+2cm)	14 (+2cm)	16 (+2cm)	18 (+2cm)	20 (+2cm)	22 (+2cm)
24 (+2cm)	26 (+2cm)	28 (+2cm)	30 (+4cm)	34 (+4cm)	38 (+4cm)
42 (+4cm)	46 (+4cm)	50 (+4cm)	54 (+4cm)	58 (+4cm)	62 (+4cm)
66 (+8cm)	74 (+8cm)	82 (+8cm)	90 (+8cm)	98 (+8cm)	106 (+8cm)
114 (+8cm)	122 (+8cm)	130 (+12cm)	142 (+12cm)	154 (+12cm)	166 (+12cm)
178 (+12cm)	190 (+12cm)	202 (+12cm)	214 (+12cm)	226 (+12cm)	238 (+12cm)
250 (+12cm)	262 (+12cm)	274 (+12cm)	286 (+8cm)	294 (+8cm)	302 (+4cm)
306 (+4cm)	310 (+4cm)	314 (+4cm)	318 (+4cm)	322 (+2cm)	324 (+2cm)
326 (+2cm)	328 (+2cm)	330 (+2cm)	332 (+2cm)	334 (+2cm)	336 (+2cm)
338 (+2cm)	340 (+2cm)	342 (+2cm)	344 (+2cm)	346 (+2cm)	348 (+2cm)
350 (+2cm)	352 (+2cm)	354 (+2cm)	356 (+2cm)	358 (+2cm)	360 (+2cm)
362 (+2cm)	364 (+2cm)	366 (+2cm)	368 (+2cm)	370 (+2cm)	372 (+2cm)
374 (+2cm)	376 (+2cm)	378 (+2cm)	380 (+2cm)	382 (+2cm)	384 (+2cm)
386 (+2cm)	388 (+2cm)	390 (+2cm)	392 (+2cm)	394 (+2cm)	396 (+2cm)
398 (+2cm)	400 (+2cm)	402 (+2cm)	404 (+2cm)	406 (+2cm)	408 (+2cm)
410 (+2cm)	412 (+2cm)	414 (+2cm)	416 (+2cm)	418 (+2cm)	420 (+2cm)
422 (+2cm)	424 (+2cm)	426 (+2cm)	428 (+2cm)	430 (+4cm)	434 (+4cm)
438 (+4cm)	442 (+4cm)	446 (+4cm)	450 (+4cm)	454 (+4cm)	458 (+4cm)
462 (+8cm)	470 (+8cm)	478 (+8cm)	486 (+12cm)	498 (+12cm)	510 (+12cm)
522 (+12cm)	534 (+12cm)	546 (+12cm)			

Table 2: Measurement locations in Z for when probe is placed at r=30.5 cm (12 inches) from the beam line. Values are in cm and measured downstream along the beamline with zero being even with the upstream face of the most upstream coil in the magnet (see figure 6).

30.5 cm (12") - 139 points					
0 (+2cm)	2 (+2cm)	4 (+2cm)	6 (+2cm)	8 (+2cm)	10 (+2cm)
12 (+2cm)	14 (+2cm)	16 (+2cm)	18 (+2cm)	20 (+2cm)	22 (+2cm)
24 (+2cm)	26 (+2cm)	28 (+2cm)	30 (+4cm)	34 (+4cm)	38 (+4cm)
42 (+4cm)	46 (+4cm)	50 (+4cm)	54 (+4cm)	58 (+8cm)	66 (+8cm)
74 (+8cm)	82 (+8cm)	90 (+8cm)	98 (+8cm)	106 (+8cm)	114 (+8cm)
122 (+8cm)	130 (+12cm)	142 (+12cm)	154 (+12cm)	166 (+12cm)	178 (+12cm)
190 (+12cm)	202 (+12cm)	214 (+12cm)	226 (+12cm)	238 (+12cm)	250 (+12cm)
262 (+12cm)	274 (+12cm)	286 (+8cm)	294 (+8cm)	302 (+4cm)	306 (+4cm)
310 (+4cm)	314 (+4cm)	318 (+2cm)	320 (+2cm)	322 (+2cm)	324 (+2cm)
326 (+2cm)	328 (+2cm)	330 (+2cm)	332 (+2cm)	334 (+2cm)	336 (+2cm)
338 (+2cm)	340 (+2cm)	342 (+2cm)	344 (+2cm)	346 (+2cm)	348 (+2cm)
350 (+2cm)	352 (+1cm)	353 (+1cm)	354 (+1cm)	355 (+1cm)	356 (+1cm)
357 (+1cm)	358 (+1cm)	359 (+1cm)	360 (+1cm)	361 (+1cm)	362 (+1cm)
363 (+1cm)	364 (+1cm)	365 (+1cm)	366 (+1cm)	367 (+1cm)	368 (+1cm)
369 (+1cm)	370 (+1cm)	371 (+1cm)	372 (+1cm)	373 (+1cm)	374 (+1cm)
375 (+1cm)	376 (+1cm)	377 (+1cm)	378 (+1cm)	379 (+1cm)	380 (+1cm)
381 (+1cm)	382 (+1cm)	383 (+1cm)	384 (+1cm)	385 (+2cm)	387 (+2cm)
389 (+2cm)	391 (+2cm)	393 (+2cm)	395 (+2cm)	397 (+2cm)	399 (+2cm)
401 (+2cm)	403 (+2cm)	405 (+2cm)	407 (+2cm)	409 (+2cm)	411 (+2cm)
413 (+2cm)	415 (+2cm)	417 (+2cm)	419 (+2cm)	421 (+2cm)	423 (+2cm)
425 (+2cm)	427 (+2cm)	429 (+2cm)	431 (+4cm)	435 (+4cm)	439 (+4cm)
443 (+4cm)	447 (+4cm)	451 (+4cm)	455 (+4cm)	459 (+8cm)	467 (+8cm)
475 (+8cm)	483 (+8cm)	491 (+12cm)	503 (+12cm)	515 (+12cm)	527 (+12cm)
539 (+12cm)					

Table 3: Measurement locations in Z for when probe is placed at r=55.9 cm (22 inches) from the beam line. Values are in cm and measured downstream along the beamline with zero being even with the upstream face of the most upstream coil in the magnet (see figure 6).

55.9 cm (22") - 169 points					
0 (+1cm)	1 (+1cm)	2 (+1cm)	3 (+1cm)	4 (+1cm)	5 (+1cm)
6 (+1cm)	7 (+2cm)	9 (+2cm)	11 (+2cm)	13 (+2cm)	15 (+2cm)
17 (+2cm)	19 (+2cm)	21 (+2cm)	23 (+2cm)	25 (+2cm)	27 (+2cm)
29 (+2cm)	31 (+2cm)	33 (+4cm)	37 (+4cm)	41 (+4cm)	45 (+8cm)
53 (+8cm)	61 (+8cm)	69 (+4cm)	73 (+4cm)	77 (+4cm)	81 (+4cm)
85 (+4cm)	89 (+4cm)	93 (+4cm)	97 (+4cm)	101 (+4cm)	105 (+8cm)
113 (+8cm)	121 (+12cm)	133 (+12cm)	145 (+12cm)	157 (+12cm)	169 (+12cm)
181 (+12cm)	193 (+8cm)	201 (+8cm)	209 (+8cm)	217 (+8cm)	225 (+8cm)
233 (+8cm)	241 (+12cm)	253 (+12cm)	265 (+8cm)	273 (+8cm)	281 (+4cm)
285 (+4cm)	289 (+4cm)	293 (+4cm)	297 (+4cm)	301 (+4cm)	305 (+4cm)
309 (+2cm)	311 (+2cm)	313 (+2cm)	315 (+2cm)	317 (+2cm)	319 (+2cm)
321 (+2cm)	323 (+2cm)	325 (+2cm)	327 (+2cm)	329 (+2cm)	331 (+2cm)
333 (+1cm)	334 (+1cm)	335 (+1cm)	336 (+1cm)	337 (+1cm)	338 (+1cm)
339 (+1cm)	340 (+1cm)	341 (+1cm)	342 (+1cm)	343 (+1cm)	344 (+1cm)
345 (+1cm)	346 (+1cm)	347 (+1cm)	348 (+1cm)	349 (+1cm)	350 (+1cm)
351 (+1cm)	352 (+1cm)	353 (+1cm)	354 (+1cm)	355 (+1cm)	356 (+1cm)
357 (+1cm)	358 (+1cm)	359 (+1cm)	360 (+1cm)	361 (+1cm)	362 (+1cm)
363 (+1cm)	364 (+1cm)	365 (+1cm)	366 (+1cm)	367 (+1cm)	368 (+1cm)
369 (+1cm)	370 (+1cm)	371 (+1cm)	372 (+1cm)	373 (+1cm)	374 (+1cm)
375 (+1cm)	376 (+1cm)	377 (+1cm)	378 (+1cm)	379 (+1cm)	380 (+1cm)
381 (+1cm)	382 (+1cm)	383 (+1cm)	384 (+1cm)	385 (+1cm)	386 (+1cm)
387 (+1cm)	388 (+1cm)	389 (+1cm)	390 (+1cm)	391 (+1cm)	392 (+1cm)
393 (+1cm)	394 (+1cm)	395 (+1cm)	396 (+1cm)	397 (+2cm)	399 (+2cm)
401 (+2cm)	403 (+2cm)	405 (+2cm)	407 (+2cm)	409 (+2cm)	411 (+2cm)
413 (+2cm)	415 (+2cm)	417 (+2cm)	419 (+2cm)	421 (+2cm)	423 (+2cm)
425 (+2cm)	427 (+2cm)	429 (+2cm)	431 (+4cm)	435 (+4cm)	439 (+4cm)
443 (+4cm)	447 (+4cm)	451 (+4cm)	455 (+4cm)	459 (+8cm)	467 (+8cm)
475 (+8cm)	483 (+12cm)	495 (+12cm)	507 (+12cm)	519 (+12cm)	531 (+12cm)
543 (+12cm)					

Table 4: Measurement locations in Z for when probe is placed at r=81.3 cm (32 inches) from the beam line. Values are in cm and measured downstream along the beamline with zero being even with the upstream face of the most upstream coil in the magnet (see figure 6).

81.3 cm (32") - 229 points					
0 (+1cm)	1 (+1cm)	2 (+1cm)	3 (+1cm)	4 (+1cm)	5 (+1cm)
6 (+1cm)	7 (+1cm)	8 (+1cm)	9 (+1cm)	10 (+1cm)	11 (+1cm)
12 (+1cm)	13 (+1cm)	14 (+1cm)	15 (+1cm)	16 (+1cm)	17 (+1cm)
18 (+1cm)	19 (+1cm)	20 (+1cm)	21 (+1cm)	22 (+1cm)	23 (+1cm)
24 (+1cm)	25 (+1cm)	26 (+1cm)	27 (+1cm)	28 (+1cm)	29 (+1cm)
30 (+1cm)	31 (+1cm)	32 (+1cm)	33 (+1cm)	34 (+1cm)	35 (+2cm)
37 (+2cm)	39 (+2cm)	41 (+2cm)	43 (+2cm)	45 (+2cm)	47 (+2cm)
49 (+2cm)	51 (+2cm)	53 (+2cm)	55 (+2cm)	57 (+2cm)	59 (+2cm)
61 (+2cm)	63 (+2cm)	65 (+2cm)	67 (+2cm)	69 (+1cm)	70 (+1cm)
71 (+1cm)	72 (+1cm)	73 (+1cm)	74 (+1cm)	75 (+1cm)	76 (+1cm)
77 (+1cm)	78 (+1cm)	79 (+1cm)	80 (+1cm)	81 (+1cm)	82 (+1cm)
83 (+1cm)	84 (+1cm)	85 (+1cm)	86 (+1cm)	87 (+1cm)	88 (+1cm)
89 (+1cm)	90 (+1cm)	91 (+1cm)	92 (+1cm)	93 (+1cm)	94 (+1cm)
95 (+1cm)	96 (+1cm)	97 (+1cm)	98 (+1cm)	99 (+2cm)	101 (+2cm)
103 (+2cm)	105 (+2cm)	107 (+2cm)	109 (+2cm)	111 (+2cm)	113 (+2cm)
115 (+4cm)	119 (+4cm)	123 (+4cm)	127 (+8cm)	135 (+8cm)	143 (+4cm)
147 (+4cm)	151 (+4cm)	155 (+4cm)	159 (+4cm)	163 (+4cm)	167 (+4cm)
171 (+4cm)	175 (+4cm)	179 (+2cm)	181 (+2cm)	183 (+2cm)	185 (+2cm)
187 (+2cm)	189 (+2cm)	191 (+2cm)	193 (+2cm)	195 (+2cm)	197 (+2cm)
199 (+1cm)	200 (+1cm)	201 (+1cm)	202 (+1cm)	203 (+1cm)	204 (+1cm)
205 (+1cm)	206 (+1cm)	207 (+1cm)	208 (+1cm)	209 (+1cm)	210 (+1cm)
211 (+1cm)	212 (+1cm)	213 (+1cm)	214 (+1cm)	215 (+1cm)	216 (+1cm)
217 (+1cm)	218 (+1cm)	219 (+1cm)	220 (+2cm)	222 (+2cm)	224 (+2cm)
226 (+2cm)	228 (+2cm)	230 (+2cm)	232 (+2cm)	234 (+2cm)	236 (+4cm)
240 (+4cm)	244 (+4cm)	248 (+4cm)	252 (+4cm)	256 (+4cm)	260 (+4cm)
264 (+2cm)	266 (+2cm)	268 (+2cm)	270 (+2cm)	272 (+2cm)	274 (+2cm)
276 (+2cm)	278 (+2cm)	280 (+2cm)	282 (+2cm)	284 (+2cm)	286 (+2cm)
288 (+1cm)	289 (+1cm)	290 (+1cm)	291 (+1cm)	292 (+1cm)	293 (+1cm)
294 (+1cm)	295 (+1cm)	296 (+1cm)	297 (+1cm)	298 (+1cm)	299 (+1cm)
300 (+1cm)	301 (+1cm)	302 (+1cm)	303 (+1cm)	304 (+1cm)	305 (+1cm)
306 (+1cm)	307 (+1cm)	308 (+1cm)	309 (+1cm)	310 (+1cm)	311 (+1cm)
312 (+1cm)	313 (+1cm)	314 (+1cm)	315 (+1cm)	316 (+1cm)	317 (+1cm)
318 (+1cm)	319 (+1cm)	320 (+1cm)	321 (+1cm)	322 (+1cm)	323 (+1cm)
324 (+1cm)	325 (+1cm)	326 (+1cm)	327 (+1cm)	328 (+1cm)	329 (+1cm)

Table 5: Continuation of table 4.

81.3 cm (32") - 229 points					
330 (+1cm)	331 (+1cm)	332 (+1cm)	333 (+1cm)	334 (+1cm)	335 (+1cm)
336 (+1cm)	337 (+1cm)	338 (+1cm)	339 (+1cm)	340 (+1cm)	341 (+1cm)
342 (+1cm)	343 (+1cm)	344 (+1cm)	345 (+1cm)	346 (+1cm)	347 (+1cm)
348 (+1cm)	349 (+1cm)	350 (+1cm)	351 (+1cm)	352 (+1cm)	353 (+1cm)
354 (+1cm)					

## 2 Required Angular Resolution

The orientation of the probe will be controlled to some level of accuracy. This means the direction of the field being measured will only be known to that level. Here, an estimate of the tolerance for the field direction is made based on the expected momentum resolution of the tracking chambers.

We start with the relation between the momentum and magnetic field as given by equation 31.49 of [4].

$$p \cos \lambda = 0.3qBR \tag{1}$$

where:

$p$  is the momentum in GeV/c

$\lambda$  is the “dip” or “pitch” angle which is just  $\frac{\pi}{2} - \theta$  ( $\theta$  being the standard polar angle)

$q$  is the charge of the particle ( $\pm 1$ )  $B$  is the magnitude of the field in Tesla

$R$  is the radius of curvature in the bending plane

The uncertainty in momentum  $\Delta p$  is given by adding the uncertainties due to the individual contributors in quadrature. (This assumes the errors in field magnitude and direction are uncorrelated.)

$$(\Delta p)^2 = \left( \frac{\partial p}{\partial B} \Delta B \right)^2 + \left( \frac{\partial p}{\partial \lambda} \Delta \lambda \right)^2 \tag{2}$$

The partial derivatives of  $p$  wrt to  $B$  and  $\lambda$  are given by the following two equations:

$$\frac{\partial p}{\partial B} = 0.3qR = \frac{p}{B} \tag{3}$$

$$\frac{\partial p}{\partial \lambda} = 0.3qBR \frac{\tan \lambda}{\cos \lambda} = p \tan \lambda \quad (4)$$

Inserting these into eqn. 2 yields:

$$\left(\frac{\Delta p}{p}\right)^2 = \left(\frac{\Delta B}{B}\right)^2 + (\tan \lambda \Delta \lambda)^2 \quad (5)$$

In the limit that relative uncertainty of the momentum comes solely from the uncertainty of the angle, one solve for  $\Delta \lambda$ :

$$\Delta \lambda \approx \left(\frac{\Delta p}{p}\right) \frac{1}{\tan \lambda} \quad (6)$$

Converting from dip angle  $\lambda$  to the more familiar polar angle  $\theta$ :

$$\Delta \theta = \left(\frac{\Delta p}{p}\right) \tan \theta \quad (7)$$

The acceptable uncertainty  $\Delta \theta$  is determined by ensuring it is not the dominate factor in the overall uncertainty of the momentum resolution. The relative uncertainty in the momentum can be estimated using some well-known formulae (see pg. 365 of [4]). This has been done for the GlueX detector geometry[5] and the results for the transverse momentum can be seen in figure 3.

A tolerance on the angle of the probe relative to the B-field is calculated by requiring that it does not increase the relative uncertainty in the transverse momentum by more than some fraction. Figures 4 and 5 show tolerances for increases in  $dp_t/p_t$  of 10% and 20% respectively. For both cases the minimum tolerance is approximately 1 mrad.



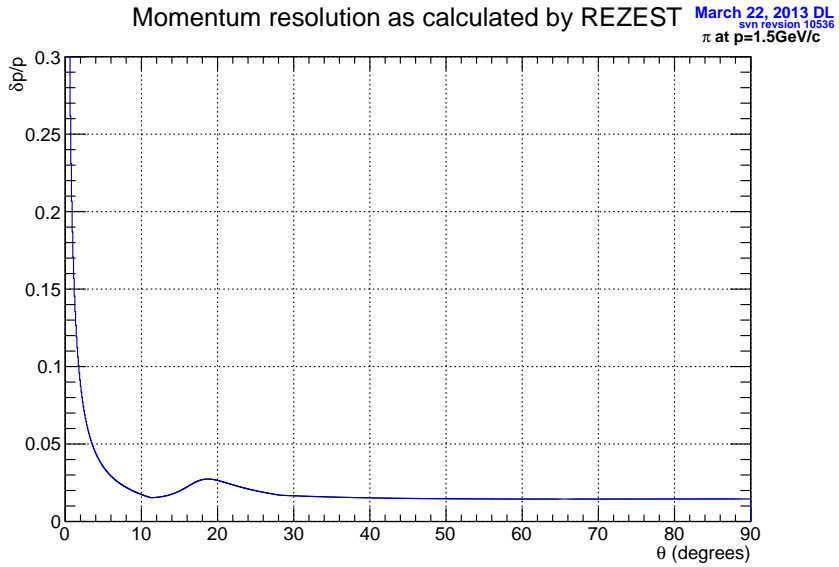


Figure 3: Transverse momentum resolution of 1.5GeV/c charged  $\pi$  in GlueX detector. This is calculated by formulas given in the references and is due to the detector materials, resolution, and spacing.

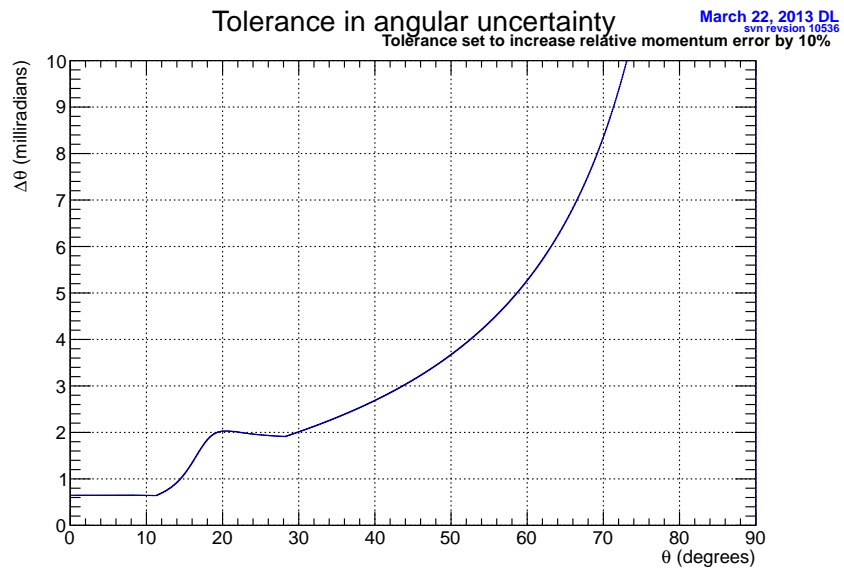


Figure 4: Tolerance in angle of probe direction relative to actual magnetic field direction leading to 10% increase in transverse momentum resolution.

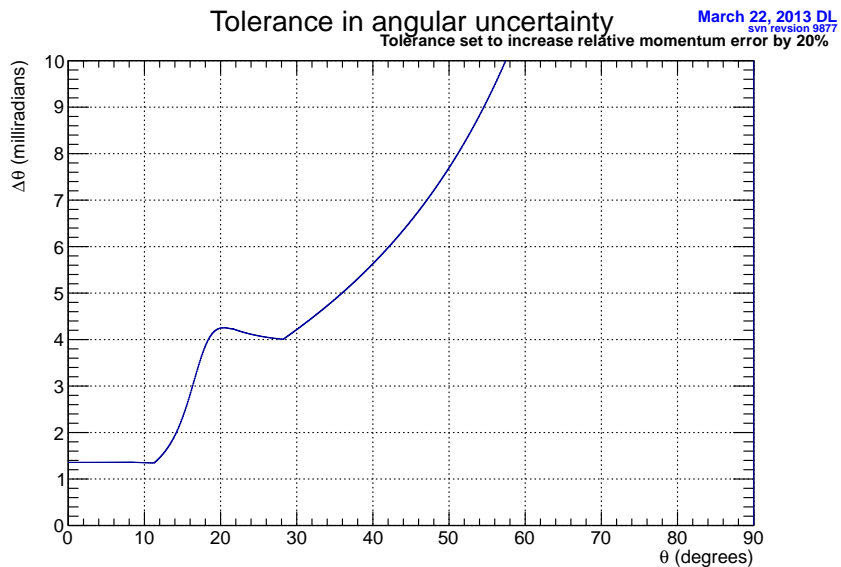


Figure 5: Tolerance in angle of probe direction relative to actual magnetic field direction leading to 20% increase in transverse momentum resolution.

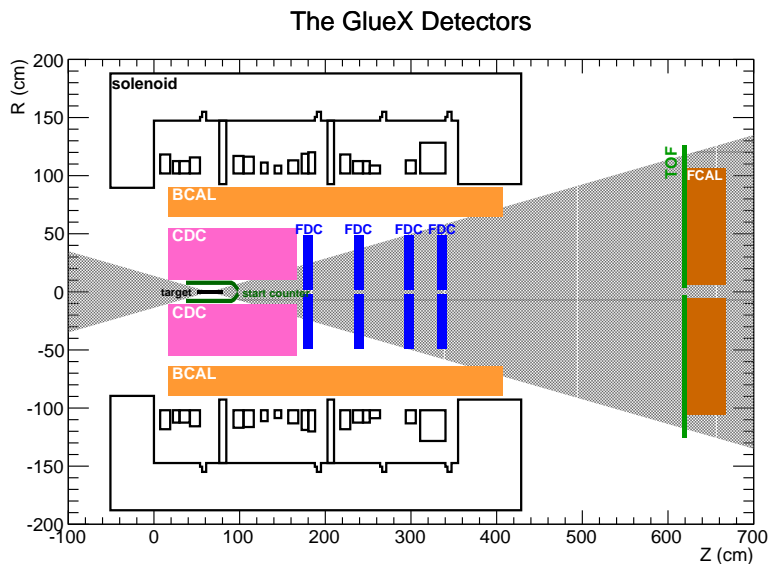


Figure 6: Schematic of GlueX detector ass seen from the side. The grey area represents areas with  $\theta \leq 12^\circ$  where an angular tolerance of 1mrad or less is desired for the probe direction. Outside of the grey regions, the tolerance is relaxed to a few or more mrad.

## References

- [1] David Lawrence. M.c. studies of gluex solenoidal field 1. Technical Report GlueX-doc-1322, Jefferson Lab, August 2009.
- [2] David Lawrence and Simon Taylor. Hall-d solenoid magnet specifications. Technical Report GlueX-doc-1552, Jefferson Lab, September 2010.
- [3] David Lawrence and Simon Taylor. Effects of field uniformity in gluex. Technical Report GlueX-doc-1556, Jefferson Lab, September 2010.
- [4] J. Beringer and et al. Review of particle physics. *Phys. Rev. D*, 86:010001, Jul 2012.
- [5] Mark Ito. A program to estimate resolution for charged particles in gluex. Technical Report GlueX-doc-1015-v2, Jefferson Lab, 2008.